scientific reports

Check for updates

OPEN

An insight into the electro-chemical properties of halogen (F, Cl and Br) doped BP and BN nanocages as anodes in metal-ion batteries

Maryam Abedi[1], Mohammad Eslami[2], Mahdi Ghadiri[3,4]✉ & Samira Mohammadinia[5]✉

Here, electro-chemical properties of BN and BP nanocages as anodes in metal-ion batteries are examined. The effect of halogens adoption of BN and BP-NCs on electro-chemical properties of M-IBs are investigated. Results showed that the BP nanocages as anode electrode in M-IBs has higher efficiency than BN nanocages and the K-IB has higher cell voltage than N-IBs. Results indicated that the halogens adoption of BN and BP-NCs are improved the cell voltage of M-IBs. Results proved that the F-doped M-IBs have higher cell voltage than M-IBs. Finally, F-$B_{17}P_{18}$ as anodes in K-IB is proposed as suitable electrodes.

In previous studies, the chemical and physical properties of boron nitride nanocages (BN-NC) and boron phosphide nanocages (BP-NC) have been investigated[1–3]. The results of previous studies confirmed that nanocages have acceptable properties as anodes and cathode materials in batteries due to low band gap energies and high potential to transfer the electrons and ions[4–7].

Results of previous studies indicated that the formation heat and formation heat of per atom of $B_{18}N_{18}$, $B_{24}N_{24}$ and $B_{36}N_{36}$ are decreased when the number of atoms are increased. Results of previous studies confirmed that the formation heat and formation heat of per atom of $B_{18}P_{18}$ is higher than those of $B_{24}P_{24}$ and $B_{36}P_{36}$, significantly[8–11]. Results of previous studies showed that the formation heat of $B_{18}N_{18}$, $B_{24}N_{24}$ and $B_{36}N_{36}$ are – 1275, – 1197 and – 1034 kcal/mol and the formation heat of per atom of $B_{18}N_{18}$, $B_{24}N_{24}$ and $B_{36}N_{36}$ are – 15, – 13 and – 12 kcal/mol[8–11].

Results of previous studies indicated that the halogen (F, Cl and Br) adoption of nanocages are decreased the band gap energies of nanocages and halogen (F, Cl and Br) adoption are improved the electro-chemical properties (cell voltage) of nanocages as anodes and cathode materials in batteries[12–15]. The potential of graphite, nanotubes and nanocages as anodes of metal-ion batteries (M-IBs) have been studied and results showed that nanocages have higher potential rather graphite and nanotubes[16–18].

In previous studies, the electro-chemical properties (cell voltage) of $B_{12}N_{12}$ as anodes in L-IBs and Na-IBs are examined and results confirmed that the F and Br are improved the properties of L-IBs and Na-IBs[19–21]. In previous studies, the metal adsorption on BN-NCs are investigated and results indicated that the lithium and potassium atoms are increased the properties of NC in M-IBs. The electronic properties of $B_{16}N_{16}$, $B_{16}P_{16}$ and $B_7C_{24}P$ are examined and and results indicated that the electro-chemical properties (cell voltage) of BN nanocages are improved by increasing the size of rigs[22,23].

Razavi et al.[24] studied the roles of halogen on potential of $B_{18}N_{18}$ and $B_{18}P_{18}$ in MIBs by theoretical methods. They demonstrated that storage capacities of $B_{18}N_{18}$ and $B_{18}P_{18}$ in L-IBs are 893 and 795 mAh/g and they showed that V_{cell} of F-doped $B_{18}N_{18}$ and $B_{18}P_{18}$ are higher than Br-doped MIBs by theoretical calculation.

Tahvili et al.[25] studied the potential of various nanocages as anodes in MIBs by theoretical methods. They indicated that $Al_{22}P_{22}$ is the suitable candidate as anode in MIBs and they showed that adsorbed halogen nanocages have higher V_{cell} than nanocages in MIBs. They proposed the F-$Al_{21}P_{22}$ nanocage as suitable material in anodes of MIBs by theoretical calculation.

[1]Department of Chemical Engineering, Faculty of Imam Mohammad Bagher, Sari Branch, Technical and Vocational University (TVU), Mazandaran, Iran. [2]Department of Electrical and Computer Engineering, Chabahar Branch, Islamic Azad University, Chabahar, Iran. [3]Institute of Research and Development, Duy Tan University, Da Nang 550000, Vietnam. [4]The Faculty of Environment and Chemical Engineering, Duy Tan University, Da Nang 550000, Vietnam. [5]Department of Chemical Engineering, Islamic Azad University, Mahshahr Branch, Mahshahr, Iran. ✉email: mahdighadiri@duytan.edu.vn; samiramohammadinia@gmail.com

In this study, electro-chemical properties of BN and BP-NCs as anodes in L-IBs, N-IBs and K-IBs are examined. The effects of F, Cl and Br doping of BN and BP-NCs on their electro-chemical properties (cell voltage) as anode electrodes in M-IBs are examined. The main goals of this study are to (1) find the cell voltages of LIBs made of BP and BN nanocages as anodes; (2) compare the cell voltages of LIBs and NIBs made of BP and BN nanocages as anodes; (3) find the effects of halogen adoption on cell voltages of LIBs made of BP and BN nanocages as anodes; (4) propose the metal-ion batteries with high cell voltage values.

Computational details

The geometries of $B_{18}N_{18}$, $B_{18}P_{18}$, X-$B_{18}N_{18}$ and X-$B_{18}P_{18}$ (X = F Cl, Br) were optimized through *DFT* method, M06-2X and HSE06 functional and 6-31G (d, p) basis set in *GAMESS*[26–30]. The DFT is described energies of inorganic–organic nanocages with acceptable accuracy and M06-2X and HSE06 functional have high accurate to estimate the energies of nano-structures[31–35]. The DFT/M06-2X is predicted the energies and frequencies of nanocages with suitable accuracy and the M06 is the best functional to estimate the vibrational frequencies of nanocages[36–40].

The adsorption of halogens (X= F Cl, Br) on nanocages and adsorption of M and M^+ on nanocages are studied. The structures of X-nanocages and M-nanocages are optimized by *DFT* method, M06-2X and HSE06 functional and 6-31G (d, p) basis set. The vibrational frequencies of studied complexes are investigated by *DFT* method, M06-2X and HSE06 functional and 6-311+G (2d, 2p) basis set[41–43].

The Gibbs free energy of structures are calculated as follow: $G = E_0 + ZPE + \Delta H_{trans} + \Delta H_{rot} + \Delta H_{vib} + RT\text{-}TS$. The Gibbs free energy of adsorption of halogens on nanocages are calculated as follow: $G_{ad} = G$ (X-nanocage) – G (nanocage) – 0.5 G (X_2). The Gibbs free energy of adsorption of M and M^+ on nanocages are calculated as follow: $G_{ad} = G$ (M-nanocage) – G (nanocage) – G (M)[44–47].

The reactions in anode and cathode of metal ion batteries are: Anode: M-nanocage ↔ M^+-nanocage + e^- and Cathode: M^+ + e^- ↔ M. The final reaction in metal-ion battery is: M^+ + M-nanocage ↔ M^+-nanocage + M. The cell voltage (V_{cell}) is calculated by via Nernst equation: $V_{cell} = -\Delta G_{cell}/zF$. The F is the Faraday constant, z is the charge of M^+ and ΔG_{cell} is $\Delta E_{cell} + P\Delta V - T\Delta S$[48–51].

Results and discussion

BN and BP as anodes in M-IBs. In this section, the structures of nanocages and complexes with halogens and metals are showed in Fig. 1. The electro-chemical properties of BN and BP-NCs as anodes in M-IBs are investigated. The structures and bond lengths (in Å) of BN and BP-NCs with metal are showed in Fig. 1.

The calculated G_{ad} of M/M^+ and BN and BP-NCs by M06-2X and HSE06 functional are summarized in Supplementary Table 1S in supplementary data. The G_{ad} values are negative and adsorption of metal on BN and BP-NCs are possible. The $|G_{ad}|$ of K-$B_{18}N_{18}$ is higher than $|G_{ad}|$ of Li-$B_{18}N_{18}$ and Na-$B_{18}N_{18}$. The $|G_{ad}|$ of adsorption of metal on $B_{18}P_{18}$ are higher than $|G_{ad}|$ on $B_{18}N_{18}$. The $|G_{ad}|$ of studied M and M^+ on BN and BP-NCs have same trends. The calculated V_{cell} of metal with BN and BP-NCs by M06-2X and HSE06 functional are reported in Table 1.

The V_{cell} of K-$B_{18}N_{18}$ is higher than Li-$B_{18}N_{18}$ and Na-$B_{18}N_{18}$ and V_{cell} of K-$B_{18}P_{18}$ is higher than Li-$B_{18}P_{18}$ and Na-$B_{18}P_{18}$. The V_{cell} of Li, Na and K on $B_{18}P_{18}$ are higher than $B_{18}N_{18}$. Here, interactions of atoms on B atom in BN and BP-NCs are examined. The structures of M atoms with BN and BP-NCs via N and P sites are showed in Fig. 1. Calculated V_{cell} of BN and BP-NCs with M atoms via N and P sites by M06-2X and HSE06 functional are reported in Table 1.

The $|G_{ad}|$ of M atoms with BN and BP-NCs via N and P sites are higher than $|G_{ad}|$ of B site ca 0.13 kcal/mol. The $|G_{ad}|$ of M^+ with BN and BP-NCs via N and P sites are higher than $|G_{ad}|$ of B site ca 0.75 kcal/mol.

The $|G_{ad}|$ of M atoms on BN and BP-NCs via N and P sites are higher than $|G_{ad}|$ of bridge B-N and B-P ca 0.28 kcal/mol. The $|G_{ad}|$ of M^+ with BN and BP-NCs via N and P sites are higher than $|G_{ad}|$ of bridge B-N and B-P site ca 1.45 kcal/mol. Results showed that the trends of calculated G_{ad} by M06-2X and HSE06 functional are same for studied nanocages.

The V_{cell} of M atoms with BN and BP-NCs via N and P sites are higher than V_{cell} of B site and bridge site ca 0.03 and 0.05 V. Finally, M atoms on BN and BP-NCs via N and P sites are more stable than B site and bridge site.

The calculated orbital energies of metal with BN and BP-NCs by M06-2X and HSE06 functional are described in Supplementary Table 2S in supplementary data. The $|E_{HOMO}|$ of metal with $B_{18}P_{18}$ are smaller than $|E_{HOMO}|$ of metal with $B_{18}N_{18}$. The E_{HLG} of K-$B_{18}N_{18}$ is smaller than E_{HLG} of Li-$B_{18}N_{18}$ and Na-$B_{18}N_{18}$.

Results show that the trends of calculated E_{HOMO}, E_{LUMO} and E_{HLG} by M06-2X and HSE06 functional are same for studied nanocages. The $B_{18}P_{18}$ in M-IBs has higher efficiency than $B_{18}N_{18}$ and KIB has higher V_{cell} than NIB and KIB.

F, Cl and Br doped BN and BP nano-structures as anodes in MIBs. The calculated G_{ad} of F-, Cl- and Br-doped BN-NCs and BP-NCs by M06-2X and HSE06 functional are summarized in Supplementary Table 1S in supplementary data. The G_{ad} values are negative and halogens adoption of BN and BP-NCs are possible, from thermodynamic view point. The $|G_{ad}|$ of X-$B_{17}N_{18}$ and X-$B_{17}P_{18}$ are higher than X-$B_{18}N_{17}$ and X-$B_{18}P_{17}$ ca 2.07 and 2.05 kcal/mol. The B atoms of BN and BP-NCs are suitable to replace with halogen atoms.

The $|G_{ad}|$ of F-$B_{17}N_{18}$ is higher than Cl-$B_{17}N_{18}$ and Br-$B_{17}N_{18}$. The $|G_{ad}|$ of F-$B_{17}P_{18}$ is higher than Cl-$B_{17}P_{18}$ and Br-$B_{17}P_{18}$. The $|G_{ad}|$ of doping of $B_{18}P_{18}$ with halogens are higher than $B_{18}N_{18}$. Doping of BN and BP-NCs with F is possible process from thermodynamic view point and F-$B_{17}N_{18}$ and F-$B_{17}P_{18}$ are acceptable candidates in M-IBs.

The structures and bond lengths of halogen doped nanocages with metals are showed in Fig. 1. The G_{ad} of M and M^+ with halogen doped nanocages are presented in Supplementary Table 1S in supplementary data. The G_{ad} values are negative and adsorption of meals on halogen doped nanocages are possible.

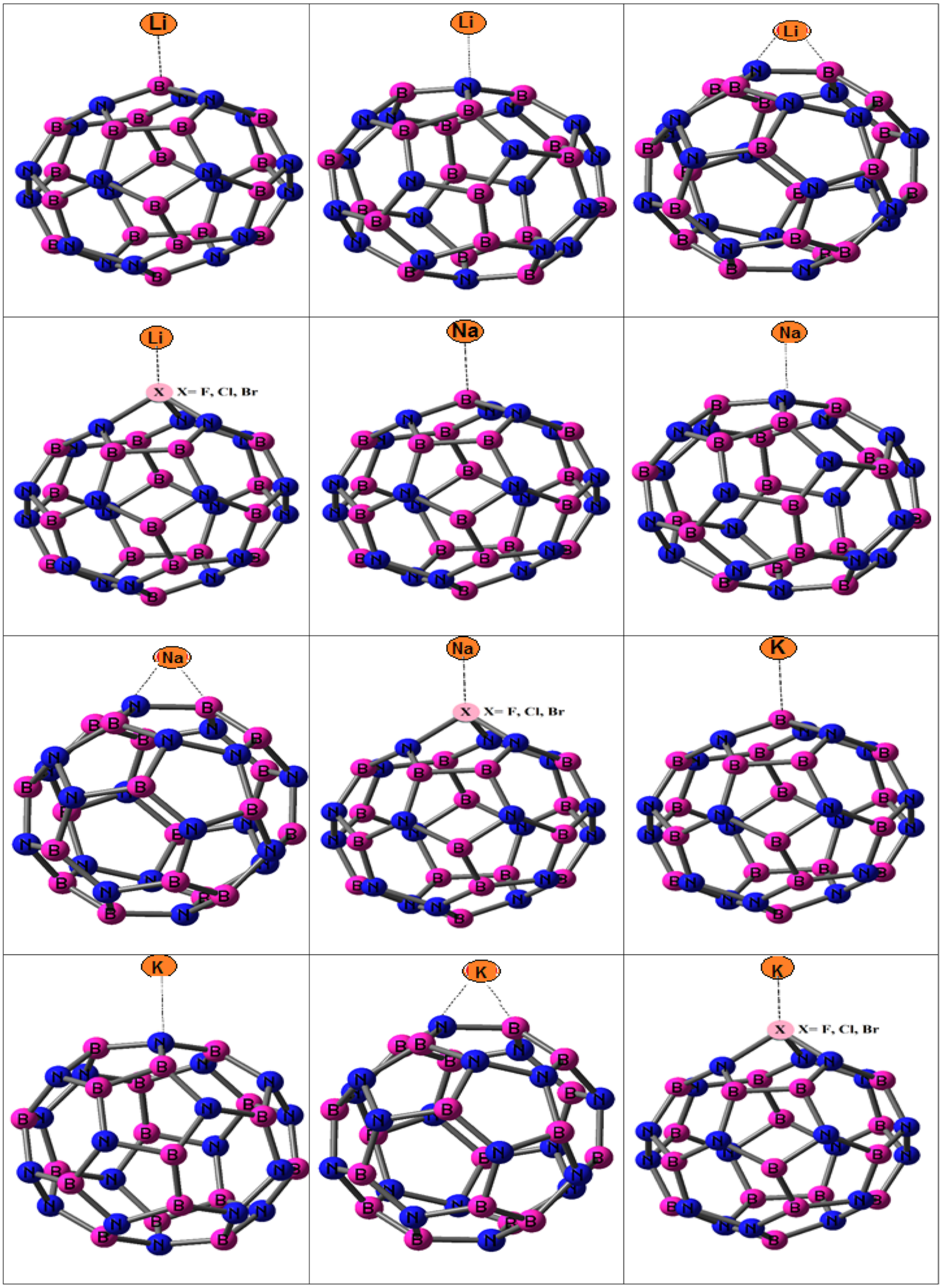

Figure 1. Structures of $B_{18}N_{18}$, $B_{18}P_{18}$, X-$B_{17}N_{18}$ and X-$B_{17}P_{18}$ with metal atoms and their bond lengths (Å) and calculated G_{ad} of adsorption of halogens on studied nanocages.

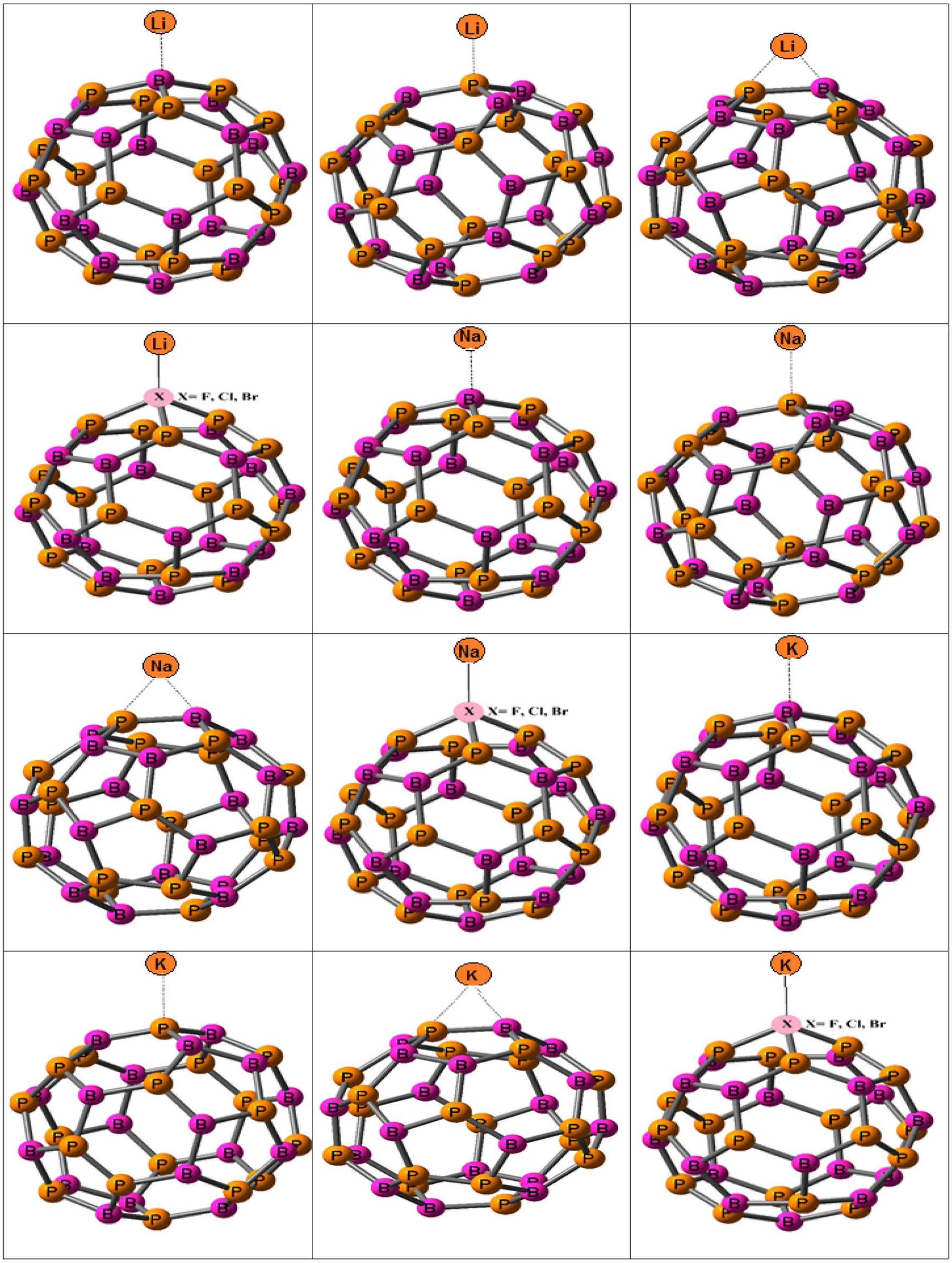

Figure 1. (continued)

The G_{ad} of K-halogen-$B_{17}P_{18}$ are higher than Na-halogen-$B_{17}P_{18}$ and Li-halogen-$B_{17}P_{18}$. The $|G_{ad}|$ of adsorption of metals on halogen-$B_{17}P_{18}$ are higher than halogen-$B_{17}N_{18}$. The $|G_{ad}|$ of F-NCs are higher than Cl-NCs and Br-NCs. The orbital energies of metals halogen doped nanocages are reported in Supplementary Table 2S in supplementary data. The $|E_{HOMO}|$ of metals with halogen-$B_{17}P_{18}$ are smaller than halogen-$B_{17}N_{18,}$ significantly.

The calculated V_{cell} of metals with halogen doped nanocages by M06-2X and HSE06 functional are reported in Table 1. The V_{cell} of K-$B_{17}N_{18}$ are higher than Li-$B_{17}N_{18}$ and Na-$B_{17}N_{18}$. The V_{cell} of K-$B_{17}P_{18}$ are higher than

Position	Complex	V_{cell} by M06-2X	V_{cell} by HSE06	Position	Structure	V_{cell} by M06-2X	V_{cell} by HSE06
B site	K-$B_{18}N_{18}$	1.39	1.43	B site	K-$B_{18}P_{18}$	1.60	1.64
B site	Na-$B_{18}N_{18}$	1.24	1.26	B site	Na-$B_{18}P_{18}$	1.43	1.45
B site	Li-$B_{18}N_{18}$	1.11	1.14	B site	Li-$B_{18}P_{18}$	1.28	1.32
N site	K-$B_{18}N_{18}$	1.41	1.44	P site	K-$B_{18}P_{18}$	1.63	1.67
N site	Na-$B_{18}N_{18}$	1.27	1.30	P site	Na-$B_{18}P_{18}$	1.45	1.48
N site	Li-$B_{18}N_{18}$	1.13	1.17	P site	Li-$B_{18}P_{18}$	1.31	1.35
Bridge B-N	K-$B_{18}N_{18}$	1.37	1.41	Bridge B-P	K-$B_{18}P_{18}$	1.57	1.62
Bridge B-N	Na-$B_{18}N_{18}$	1.22	1.26	Bridge B-P	Na-$B_{18}P_{18}$	1.41	1.45
Bridge B-N	Li-$B_{18}N_{18}$	1.08	1.11	Bridge B-P	Li-$B_{18}P_{18}$	1.25	1.29
K-F-$B_{17}N_{18}$		3.12	3.22	K-F-$B_{17}P_{18}$		3.59	3.70
Na-F-$B_{17}N_{18}$		2.78	2.87	Na-F-$B_{17}P_{18}$		3.20	3.30
Li-F-$B_{17}N_{18}$		2.49	2.57	Li-F-$B_{17}P_{18}$		2.86	2.96
K-Cl-$B_{17}N_{18}$		2.95	3.04	K-Cl-$B_{17}P_{18}$		3.39	3.50
Na-Cl-$B_{17}N_{18}$		2.64	2.70	Na-Cl-$B_{17}P_{18}$		3.03	3.11
Li-Cl-$B_{17}N_{18}$		2.35	2.45	Li-Cl-$B_{17}P_{18}$		2.71	2.82
K-Br-$B_{17}N_{18}$		2.78	2.89	K-Br-$B_{17}P_{18}$		3.20	3.33
Na-Br-$B_{17}N_{18}$		2.49	2.58	Na-Br-$B_{17}P_{18}$		2.86	2.96
Li-Br-$B_{17}N_{18}$		2.22	2.29	Li-Br-$B_{17}P_{18}$		2.55	2.64

Table 1. The calculated V_{cell} of BN and BP nanostructures.

Li-$B_{17}P_{18}$ and Na-$B_{17}P_{18}$. The V_{cell} of metals with halogen-$B_{17}P_{18}$ are higher than metals with halogen-$B_{17}N_{18}$. Results show that the trends of calculated V_{cell} by M06-2X and HSE06 functional are same for studied nanocages.

In present paper, F doping of BN and BP-NCs is increased the V_{cell} of them in M-IBs. The V_{cell} of F-$B_{17}N_{18}$ and F-$B_{17}P_{18}$ in N-IB are higher than V_{cell} of F-$B_{17}N_{18}$ and F-$B_{17}P_{18}$ in L-IB. The halogens doping of NCs are increased the V_{cell} of M-IBs. The K-ion batteries have higher V_{cell} than M-IBs and the K-F-$B_{17}P_{18}$ in M-IBs has the highest V_{cell}.

Conclusion

In this study, the electro-chemical properties of BN and BP-NCs as anodes in M-IBs are examined. The roles of halogens adoption on electro-chemical properties of BN-NCs and BP-NCs as anodes of metal-IB are investigated. The obtained results of this study are: (1) the $B_{18}P_{18}$ as anode electrode of M-IBs has higher efficiency than $B_{18}N_{18}$; (2) the KIB has higher V_{cell} than NIB and KIB; (3) halogens are increased V_{cell} in M-IBs; (4) the F doped NCs have higher V_{cell} than Cl and Br doped NCs in M-IBs; (5) F-$B_{17}P_{18}$ has the highest V_{cell} as anode electrodes in K-IB and F-$B_{17}P_{18}$ is proposed as novel anodes in M-IBs.

Data availability

The calculated G_{ad} of nano-structures by M06-2X and HSE06 functional are presented in Table 1S and calculated energies of orbitals and q of nano-structures by M06-2X and HSE06 functional are presented in Table 2S.

Received: 14 August 2020; Accepted: 2 November 2020
Published online: 17 November 2020

References

1. Chao, W. Thermal lithiated-TiO_2: A robust and electron-conducting protection layer for Li–Si alloy anode. *ACS Appl. Mater. Inter.* **10**, 12750–12758 (2018).
2. Jie, Z. Surface fluorination of reactive battery anode materials for enhanced stability. *J. Am. Chem. Soc.* **139**, 11550–11558 (2017).
3. Eunjoo, Y. Cycle stability of rechargeable Li–O_2 batteries by the synergy effect of a LiF protective layer on the Li and DMTFA additive. *ACS Appl. Mater. Interfaces.* **9**, 21307–21313 (2017).
4. Xuemin, L. Study of lithium silicide nanoparticles as anode materials for advanced lithium ion batteries. *ACS Appl. Mater. Interfaces.* **9**, 16071–16080 (2017).
5. Daniel, H. Feasibility of full (Li-Ion)–O_2 cells comprised of hard carbon anodes. *ACS Appl. Mater. Interface.* **9**, 4352–4361 (2017).
6. Si, H. Exploring real-world applications of electrochemistry by constructing a rechargeable lithium-ion battery. *Nano. Lett.* **15**, 8122–8128 (2015).
7. Oku, T. Additional emissions and cost from storing electricity in stationary battery systems. *Diam. Relat. Mater.* **12**, 840–845 (2003).
8. Alexandre, S. S., Chacham, H. & Nunes, R. W. Structure and energetics of boron nitride fullerenes: The role of stoichiometry. *Phys. Rev. B* **63**, 45402–45409 (2001).
9. Sun, M. L., Slanina, Z. & Lee, S. L. A theoretical study of BN nanocages. *Chem. Phys. Lett.* **233**, 279–284 (1995).
10. Fowler, P. W., Terrones, M. & Terrones, H. Quantum-chemical calculations of the piezoelectric characteristics of boron nitride and carbon nanocages. *Chem. Phys. Lett.* **299**, 359–368 (1999).
11. Alexandre, S. S., Nunes, R. W. & Chacham, H. Boron nitride analogs of fullerenes, nanotubes, and fullerites. *Phys. Rev. B* **66**, 85406–85412 (2002).
12. Oku, T. Comparative life-cycle assessment of Li-Ion batteries through process-based and integrated hybrid approaches. *Mater. Manuf. Process* **19**, 1215–1239 (2004).

13. Han, L. Predicting structure and electrochemistry of dilithium thiophene-2,5-dicarboxylate electrodes by density functional theory and evolutionary algorithms. *Nanotechnology.* **28**, 701–706 (2017).
14. Hosseini, J. First-principles density functional theory modeling of Li binding: Thermodynamics and redox properties of quinone derivatives for lithium-ion batteries. *J. Mol. Liq.* **225**, 913–918 (2017).
15. Najafi, M. Impact of recycling on cradle-to-gate energy consumption and greenhouse gas emissions of automotive lithium-ion batteries. *Can. J. Chem.* **95**, 687–690 (2017).
16. Nejati, K. Potential environmental and human health impacts of rechargeable lithium batteries in electronic waste. *J. Mol. Graph. Mod.* **74**, 1–7 (2017).
17. Hosseinian, A. Recycling technologies of nickel–metal hydride batteries: An LCA based analysis. *Phys. Lett. A* **381**, 2010–2015 (2017).
18. Soltani, A. Life cycle assessment of lithium nickel cobalt manganese oxide (NCM) batteries for electric passenger vehicles. *J. Phys. Chem. Solids* **75**, 1099–1105 (2014).
19. Wu, H. Environmental and economic optima of solar home systems design: A combined LCA and LCC approach. *Int. J. Hydrog. Energy* **37**, 14336–14341 (2012).
20. Ayub, K. Flow battery production: Materials selection and environmental impact. *J. Mater. Chem. C* **4**, 10919–10934 (2016).
21. Kalateh, K. An aqueous conducting redox-polymer-based proton battery that can withstand rapid constant-voltage charging and sub-zero temperatures. *Int. J. New Chem.* **2**, 213–222 (2015).
22. Fowler, P. W. Life cycle assessment of electric vehicle batteries: An overview of recent literature. *J. Chem. Soc.* **92**, 2197–2201 (1996).
23. Razavi, R., Najafi, M., Rajabiyoun, N. & Tahvili, A. Examination of properties of nanocages (B18N18 and B18P18) as anode electrodes in metal-ion batteries. *Chem. Phys.* **522**, 279–284 (2019).
24. Razavi, R., Abrishamifar, S. M., Rajaei, G. E., Kahkha, M. R. R. & Najafi, M. Theoretical investigation of the use of nanocages with an adsorbed halogen atom as anode materials in metal-ion batteries. *J. Mol. Mod.* **24**, 64–68 (2018).
25. Moon, W. H. Tuning the electrochemical properties of organic battery cathode materials: Insights from evolutionary algorithm DFT calculations. *Appl. Surf. Sci.* **253**, 7078–7081 (2007).
26. Shangqian, Z. Failure analysis of pouch-type Li–O_2 batteries with superior energy density. *J. Energy Chem.* **45**, 74–82 (2020).
27. Weihua, W. A highly efficient biomass based electrocatalyst for cathodic performance of lithium–oxygen batteries: Yeast derived hydrothermal carbon. *Electrochim. Acta* **1**, 136–139 (2020).
28. Chen, C. Improvement of lithium anode deterioration for ameliorating cyclabilities of non-aqueous Li–CO_2 batteries. *Nanoscale* **12**, 8385–8396 (2020).
29. Ruiz, V. G. Environmental feasibility of secondary use of electric vehicle lithium-ion batteries in communication base stations. *Phys. Rev. Lett.* **108**, 146103–146107 (2012).
30. Zhao, Y. Environmental impacts of lithium production showing the importance of primary data of upstream process in life-cycle assessment. *Theor. Chem. Acc.* **120**, 215–219 (2008).
31. Ireta, J., Samuel, C., Fabrice, M. & Gian, A. B. Bridging tools to better understand environmental performances and raw materials supply of traction batteries in the future EU fleet. *J. Phys. Chem. A* **108**, 5692–5699 (2004).
32. Mahmood, A. & Michel, N. Li-ion batteries: A review of a key technology for transport decarbonization. *Phys. Chem. Chem. Phys.* **87**, 1–7 (2014).
33. Wheeler, S. E. Research gaps in environmental life cycle assessments of lithium ion batteries for grid-scale stationary energy storage systems: End-of-life options and other issues. *J. Phys. Chem. A* **113**, 10376–10382 (2009).
34. Hohenstein, E. G. Trends in life cycle greenhouse gas emissions of future light duty electric vehicles. *J. Chem. Theory Comput.* **4**, 1996–2001 (2008).
35. Zhao, Y. Titanium-anthraquinone material as a new design approach for electrodes in aqueous rechargeable batteries. *Theor. Chem. Acc.* **120**, 215–241 (2008).
36. Schultz, N. E. Globally regional life cycle analysis of automotive lithium-ion nickel manganese cobalt batteries. *J. Phys. Chem. A* **109**, 4388–4403 (2005).
37. Yu, H. S. Comparative life cycle assessment of lithium-IB chemistries for residential storage. *Chem. Sci.* **7**, 5032–5051 (2016).
38. Peverati, R. Recent progress on zinc-ion rechargeable batteries. *J. Phys. Chem. Lett.* **3**, 117–124 (2011).
39. Peverati, R. Environmental and preliminary cost assessments of redox flow batteries for renewable energy storage. *Phys. Chem. Chem. Phys.* **14**, 13171–13174 (2012).
40. Sun, J. Energy use for GWh-scale lithium-IB production. *Phys. Rev. Lett.* **111**, 106401–106407 (2013).
41. Sun, J. Environmental and economic evaluation of remanufacturing lithium-ion batteries from electric vehicles. *J. Chem. Phys.* **138**, 113–118 (2013).
42. Yu, H. S. What are the energy and environmental impacts of adding battery storage to photovoltaics? A generalized life cycle assessment. *Phys. Chem. Chem. Phys.* **17**, 12146–12160 (2015).
43. Ruiz, V. G. Reducing the climate change impacts of lithium-ion batteries by their cautious management through integration of stress factors and life cycle assessment. *Phys. Rev. Lett.* **108**, 146103–146107 (2012).
44. Zhao, T. H., Patrick, B., George, P. D. & Karim, Z. Progress and status of hydrometallurgical and direct recycling of Li-Ion batteries and beyond. *J. Phys. Chem. A* **104**, 9062–9065 (2000).
45. Ulderico, U. Low-polarization lithium-oxygen battery using ionic liquid electrolyte. *Chemsuschem* **11**, 229–236 (2018).
46. Tao, Z. A lithium-ion oxygen battery with a Si anode lithiated in situ by a Li 3 N-containing cathode. *Chem. Commun.* **54**, 1069–1072 (2018).
47. Zhang, P. Peptide-based nanoprobes for molecular imaging and disease diagnostics. *Chem. Soc. Rev.* **47**, 3490–3529 (2018).
48. Peng, Z. Functional and stability orientation synthesis of materials and structures in aprotic Li–O_2 batteries. *Chem. Soc. Rev.* **47**, 2921–3004 (2018).
49. Luo, K. Enhanced cycling stability of Li–O_2 batteries by using a polyurethane/SiO_2/glass fiber nanocomposite separator. *J. Mater. Chem. A* **6**, 7770–7776 (2018).
50. Guo, Z. A flexible polymer-based Li–air battery using a reduced graphene oxide/Li composite anode. *J. Mater. Chem. A* **6**, 6022–6032 (2018).
51. Giridhar, P. Electrodeposition of Lithium-Silicon Alloys from 1-butyl-1-methylpyrrolidinium bisamide. *J. Electrochem. Soc.* **165**, 790–795 (2018).

Author contributions

S.M. wrote the first version of paper. M.A., M.E., and M.G. collaborated in revision.

Competing interests

The authors declare no competing interests.

Additional information

Supplementary information is available for this paper at https://doi.org/10.1038/s41598-020-76749-0.

Correspondence and requests for materials should be addressed to M.G. or S.M.